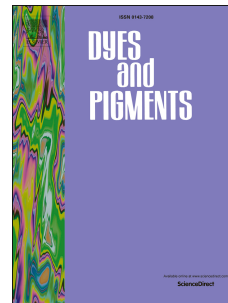


Accepted Manuscript

Effective Management of Intramolecular Charge Transfer to Obtain from Blue to Violet-blue OLEDs Based on a Couple of Phenanthrene Isomers

Xinhua Ouyang, Xiang-Long Li, Xingye Zhang, Amjad Islam, Ziyi Ge, Shi-Jian Su



PII: S0143-7208(15)00254-5

DOI: [10.1016/j.dyepig.2015.06.036](https://doi.org/10.1016/j.dyepig.2015.06.036)

Reference: DYPI 4838

To appear in: *Dyes and Pigments*

Received Date: 3 April 2015

Revised Date: 19 June 2015

Accepted Date: 22 June 2015

Please cite this article as: Ouyang X, Li X-L, Zhang X, Islam A, Ge Z, Su S-J, Effective Management of Intramolecular Charge Transfer to Obtain from Blue to Violet-blue OLEDs Based on a Couple of Phenanthrene Isomers, *Dyes and Pigments* (2015), doi: 10.1016/j.dyepig.2015.06.036.

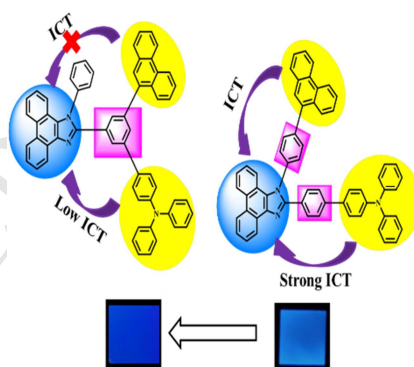
This is a PDF file of an unedited manuscript that has been accepted for publication. As a service to our customers we are providing this early version of the manuscript. The manuscript will undergo copyediting, typesetting, and review of the resulting proof before it is published in its final form. Please note that during the production process errors may be discovered which could affect the content, and all legal disclaimers that apply to the journal pertain.

Effective Management of Intramolecular Charge Transfer to Obtain from Blue to Violet-blue OLEDs Based on a Couple of Phenanthrene Isomers

Keywords: Violet-blue emission, Intramolecular charge transfer, Phenanthrene isomers

Xinhua Ouyang¹, Xianglong Li², Xingye Zhang¹, Amjad Islam¹, Shijian Su^{2*}, Ziyi Ge^{1*}

A couple of phenanthrene isomers (PATPA) were designed and synthesized by introducing strong D- π -A structure strategy to manage effectively their intramolecular charge transfer (ICT) processes for violet-blue emitters.



Effective Management of Intramolecular Charge Transfer to Obtain from Blue to Violet-blue OLEDs Based on a Couple of Phenanthrene Isomers

Xinhua Ouyang¹, Xiang-Long Li², Xingye Zhang¹, Amjad Islam¹, Ziyi Ge^{1*}, Shi-Jian Su^{2*},

¹*Ningbo Institute of Materials Technology and Engineering, Chinese Academy of Sciences, Ningbo 315201, P.R. China*

²*State Key Laboratory of Luminescent Materials and Devices (South China University of Technology) and Institute of Polymer Optoelectronic Materials and Devices, South China University of Technology, Guangzhou 510640, P.R. China*

Corresponding authors: gezzyi@nimte.ac.cn (Z. Ge), mssjsu@scut.edu.cn (S. Su)

Abstract: A couple of phenanthrene isomers were designed and synthesized by introducing strong D- π -A structure strategy to manage effectively their intramolecular charge transfer processes for violet-blue emitters. Their physical properties, including UV-vis, photoluminescence, thermal and electrochemistry, were systematically studied. The results were found to be good candidates as emitters for organic light emitting diodes (OLEDs). The devices based on them exhibit deep-blue light emissions with CIE coordinates of (0.15, 0.15) for p-PATPA and violet-blue (0.16, 0.05) for m-PATPA at 100 cd/m², respectively. The violet-blue device shows good performance with external quantum efficiency (EQE), current efficiency (CE), and power efficiency (PE) of 2.39%, 0.78 cd/A, and 0.72 lm/W, respectively. Furthermore, at the high luminescence, the device still indicated good performance with relative

low efficiency roll-off. Our results here successfully provide an efficient design strategy with strong donor and acceptor for violet-blue emitters.

Keywords Violet-blue emission, Intramolecular charge transfer, Phenanthrene isomers

Introduction

Blue organic light-emitting diodes (OLEDs) have been attracting extensively attention from scientific and industrial fields due to the importance in flat-panel displays (FPD) and solid-state lighting (SSL) resources.^[1-3] Generally, a high color saturation or color rendering index of white OLEDs requires at least a deep-blue emission with a Commission Internationale de l'Eclairage (CIE) y coordinate value of less 0.10.^[4] The development of deep-blue, even violet-blue materials, is of special significance because such emitters can not only effectively reduce the power consumptions of FPD and SSL, but also be utilized to generate light of other colors by energy cascade to a lower-energy fluorescent or phosphorescent.^[5]

In the past decades, numerous compounds have been developed to be used as blue emitters, and some of them exhibited good performance.^[6] However, the present compounds with violet-blue or violet emission are still very rare. In view of this, the research about the violet-blue emitters with high performance is still the active field of OLEDs.^[7] Due to the larger HOMO-LUMO gap, the design and synthesis of this are still the challenges for us. Recently, some researchers put forward the thought of introduction donor- π -acceptor type molecules to obtain highly-efficient violet-blue emitters.^[8] The effective method is to choose some weak electron-donating (D) and

accepting (A) units to reduce the ability of intramolecular charge transfer.^[9] Thus, it will lead to many functional groups with high fluorescent yields which cannot be introduced owing to their large π conjugation, such as anthracene,^[10] fluorene,^[11] styrylarylene^[12] and pyrene^[13] derivatives and so forth. Furthermore, the weak D- π -A type emitters will either decrease the fluorescent quantum yield and charge-transporting ability,^[14] or to some extent increase the synthetic difficulty when large molecular weight and/or bulky structure are usually required for good thermal and morphological stability.^[15] Therefore, if the D-A type emitters containing strong D and A units also can be used as highly efficiency violet-blue emission by effective management of their intramolecular charge transfer (ICT), it will be the best choice to develop the violet-blue OLEDs. Unfortunately, to our best knowledge, the violet-blue OLEDs with strong D and A units have not been reported to date.

Herein, we demonstrate a couple of phenanthrene derivatives, which contain the strong electron-donating triphenylamine (TPA) unit and electron-accepting imidazole unit, 3'-(phenanthren-9-yl)-N,N-diphenyl-5'-(1-phenyl-1H-phenanthro [9,10-d]imidazol-2-yl)-[1,1'-biphenyl]-4-amine (m-PTPAPI) and 4'-(1-(4- (phenanthren-9-yl)phenyl)-1H-phenanthro[9,10-d]imidazol-2-yl)-N,N-diphenyl-[1,1'-biphenyl]-4-amine (p-PTPAPI) (Scheme 1). As shown in the Scheme 1, it is particularly intriguing to compare the electroluminescent properties of m-PTPAPI and p-PTPAPI, both have the same molecular constructing D, A and π -conjugating units. We only changed the connecting mode of π -conjugating linkers between the D and A units from *para*- to *meta*-position. Their electronic transitions of the charge-transfer (CT) excited states

can effectively managed. The corresponding electroluminescence based on them as non-doped OLEDs emitter shows from deep-blue to blue-violet emission. The OLEDs based on m-PTPAPI as emitter achieved an external quantum efficiency of 2.39 % and a deep-blue CIE(x,y) of (0.15, 0.05), which was the first time to obtain a blue-violet emitter with strong D (TPA) and A (imidazole) units in a nondoped system to our knowledge.

Results and discussion

Synthesis As shown in Scheme1, the synthetic processes of m-PTPAPI and p-PTPAPI are similarly by three synthetic steps with good yields. The important intermediate for the synthesis of m-PTPAPI was 4'-(diphenylamino)-5-(phenanthren-9-yl)-[1,1'-biphenyl]-3-carbaldehyde (**3**), which was synthesized by two steps of Suzuki couplings from 3,5-dibromobenzaldehyde, (4-(diphenylamino)phenyl)boronic acid and phenanthren-9-ylboronic acid using Pd(PPh₃)₂Cl₂ as catalysis. While the compound p-PTPAPI was synthesized through a Suzuki coupling with 4'-(1-(4-bromophenyl)-1H-phenanthro[9,10-d]imidazol-2-yl)-N,N- diphenyl-[1,1'- biphenyl]-4-amine (**5**) and phenanthren-9-ylboronic acid. 4'-(diphenylamino)-[1,1'-biphenyl]-4-carbaldehyde (**4**) was synthesized followed the method reported literature.^[16] The compound **5** was prepared from 4'-(diphenylamino)-[1,1'-biphenyl]-4-carbaldehyde, phenanthrene-9,10-dione and 4-bromoaniline. All of new compounds were characterized using mass spectrometry, ¹H NMR, ¹³C NMR spectroscopy, and elemental analysis.

Thermal and electrochemical properties The thermal properties of m-PTPAPI and p-PTPAPI were studied by thermogravimetric analysis (TGA) and differential scanning calorimetry (DSC) under a nitrogen atmosphere with a rate of 10 °C min⁻¹. As shown in Fig. 1, their decomposition temperatures (T_d , corresponding to 5% weight loss) are 475 °C (m-PTPAPI) and 478 °C (p-PTPAPI), respectively. No obvious glass transition temperatures (T_g) are observed for them. Obviously, the T_d of p-PTPAPI are higher than that of m-PTPAPI, which indicates the introduction of *para*-configuration will improve the morphological stability. The high T_d values indicate that these molecules are stable and have the potential to be fabricated into devices by vacuum thermal evaporation technology. The electrochemical properties of them were measured by cyclic voltammetry with three electrodes system. As shown in Fig. 2, both of them exhibit similar oxidation and reduction processes. In the cathodic scan, m-PTPAPI and p-PTPAPI appeared the oxidation processes originating from their p-type TPA unit. Thus, they exhibited similar HOMO energy levels of about -5.30 eV. The LUMO levels of the two materials were calculated to be about -2.57 eV for p-PTPAPI, -2.4 eV for m-PTPAPI, respectively. Although both of them have the same reduction imidazole unit, the LUMO level of p-PTPAPI is 0.17 eV higher than that of m-PTPAPI, the imidazole is designed as *para*-configuration, which makes reduction occur more easily. The values found for the energy band gap (E_g^{ec}) of PTPAPI using cyclic voltammetry according to the equation $E_g^{ec} = (\text{HOMO-LUMO})$ are 2.73 eV and 2.90 eV for p-PTPAPI and m-PTPAPI, respectively. The higher electrochemical band gap is found to be the energy barrier of charge transfer at the

electrodes during electrochemical measurements.^[17]

Photophysical Properties Photophysical properties of PTPAPI were studied by using ultraviolet-visible (UV-vis) and photoluminescence (PL) spectrometers. The results are shown in Fig. 3 and summarized in Table 1. As shown in the absorption, the different absorptive profiles are found, the compound m-PTPAPI appears only one strong peak in chloroform and film at ~310 nm and a shoulder at ~350 nm. While the corresponding p-PTPAPI appears two absorption peaks at ~305 and ~370 nm. Obviously, the absorption at ~370 nm is ascribed to the ICT transition, and the peak at ~305 nm is from the triphenylamine-centered n- π^* transition.^[18] By comparison with the absorption of them, the charge transfer absorption band from the electron donor to the electron-withdrawing imidazole in m-PTPAPI is much lower than that of p-PTPAPI, indicating the *meta*-configuration will be benefit to prevent or reduce the charge transfer from D to A units. From the film onset absorptions, both of the band gaps (E_g) of PTPAPI are determined to be 3.15 eV for m-PTPAPI and 2.92 eV for p-PTPAPI, respectively. As shown in photoluminescent (PL) spectra, m-PTPAPI exhibits a narrow emission around 410 nm with a FWHM (full width at half maximum) of 51 nm, while p-PTPAPI shows a relatively red-shifted emission at 446 nm with a FWHM of 65 nm. Therefore, the film fluorescent emissions of both compounds are located in the short-wavelength spectral region of the whole visible light spectrum. Their ICT characteristics are studied by increasing the polarity of solvents, the gradually red-shifted and broadened fluorescent emissions are found as shown in Fig. 4, which shows a large increase of the dipole moment from the ground

state to the excited state.^[19] By calculating with the Lippert–Mataga^[20] theory, the value is 34.5 D for p-PTPAPI and 17.6 D for m-PTPAPI, The value of p-PTPAPI is larger than that of m-PTPAPI, further reflecting the ICT process in p-PTPAPI is stronger than that of m-PTPAPI.

Theoretical Calculation. To gain insight into the electronic structures of the compounds, a DFT calculation was performed at the B3LYP/6-31G (d) level. As is shown in Fig. 5, the HOMO level of m-PTPAPI mainly populate on the TPA moiety and on the linkers, while the corresponding p-PTPAPI mainly locate on the TPA and imidazole moieties. Obviously, by changing the mode of connection, a large difference of electronic density is found. In comparison of the compound of m-PTPAPI, the TPA moiety contributes less to the HOMO energy in p-PATPA. According to DFT simulation results, m-PTPAPI seems ambipolar with the separated HOMO and LUMO on donor and acceptor, respectively, while the HOMO of p-PTPAPI partially extended to imidazole group. So, the bathochromic shift of p-PTPAPI's emission should be attributed to conjugation extension of its para-linked diphenylene. The calculated HOMO level is 4.88 eV for m-PTPAPI and 4.89 eV for p-PTPAPI, suggesting that the change at the mode of connection does not have significant effect on the HOMO energy of the compounds. The LUMO levels mostly populate on the phenanthrene and the linkers between the donor and the acceptor. It is noted that both of LUMO and HOMO show a little overlapping; on one hand it would contribute for the balanced charge transfer as the emitter in OLED, but on the other hand it could facilitate the charge transfer process upon excitation, which was also

confirmed by the solvatochromic phenomenon observed in the solvent with a different polarity.^[21]

Electroluminescence (EL) properties. To investigate the EL performance of PTPAPI, non-doped fluorescent OLEDs were fabricated with a configuration of ITO/HATCN (5 nm)/NPB (x nm)/TCTA (5 nm)/PTPAPI (y nm)/TPBi (z nm)/LiF (1 nm)/Al (90 nm). In order to fully exhibit their EL performance as emitters, we regulated the thickness of NPB, PTPAPI and TPBi. In these devices, indium tin oxide (ITO) is used as the anode, hexaazatriphenylenehexacarbonitrile (HATCN) used as the hole injection layer, N,N'-di-1-naphthyl-N,N'-diphenylbenzidine (NPB) as hole-transporting layer, 4,4',4''-tri(N-carbazolyl)-triphenylamine (TCTA) as electron-blocking layer, 1,3,5-tri(phenyl-2-benzimidazolyl)benzene (TPBi) as electron-transporting and hole-blocking layer, and LiF used as the electron injecting layer. Some of important performance parameters of these OLEDs are summarized in Table 2.

By comparing to the performance of these devices, it can be seen that the device with the structure of ITO/HATCN (5 nm)/NPB (40 nm)/TCTA (5 nm)/PATPA (20 nm)/TPBi (40 nm)/LiF (1 nm)/Al (100 nm) gives the best performance in terms of luminescent (η_c), power (η_p), and external quantum (η_e) efficiencies. In particular, the efficiencies (η_e , η_p , η_e) based on p-PATPA of respectively 3.73 cd/A, 3.47 lm/W, and 3.71% were obtained. The device also has a low onset voltage (defined as the voltage required to obtain a luminance of 1 cd/m²) of 3.2 V and low operating voltages (4.2 and 5.7 V, respectively, to give a luminance of 100 and 1000 cd/m²). All of p-PTPAPI-based devices exhibit the steady deep blue emission of CIE coordinates

(0.15, 0.15) (peaked at 450 nm). While the corresponding m-PTPAPI-based devices show the similar trend except that the emission is violet-blue with the CIE coordinates (0.15, 0.05) (peaked at 408 nm).

The EL spectra of the devices with the best performance at different driving voltages were shown in Fig. 6, the present EL spectra are identical to the corresponding PL spectra of their neat films and show little change under different driving voltages, implying a good confinement of excitons in the emission layers. It can be attributed to the wide band gaps of the adjacent TCTA (3.4 eV) and TPBi (3.5 eV). The current density–voltage–luminescence (J - V - L) and brightness–efficiencies relationships by using them as emitters are shown in Fig. 7. From the current density–voltage–luminescence (J - V - L) plots, it can be seen that the PTPAPI-devices exhibit low turn-on voltages of 3.2 V, as well as much higher current densities under the same voltage as compared to the m-PTPAPI devices. These might be owing to the better charge-transporting ability of p-PTPAPI. However, the m-PTPAPI-based device exhibits relatively lower efficiencies with maximum EQE of 2.39%, CE of 0.78 cd/A, and PE of 0.72 lm/W, while the device based on p-PTPAPI presents impressive EL performance with high maximum EQE, CE, and PE of 3.71%, 3.73 cd/A and 3.47 lm/W, respectively. Notably, the CE and PE in this work based on m-PATPA show the CIE $y < 0.05$ (Table 2), which is violet-blue emission. Meanwhile, even at the practical luminescence of 1000 cd/m², the EQE and CE of the m-PTPAPI device still remain high as 2.1% and 0.69 cd/A, indicative of a relatively low efficiency roll-off. It is noteworthy that internal quantum efficiency (IQE) of the

device based on p-PTPAPI and m-PTPAPI reaches 29.7% and 25.9 % by the Monkman's theory^[22], which exceed the limit of traditional fluorescent OLEDs. It can be attributed to mechanism of hybridized local and charge-transfer (HLCT), which has been demonstrated by Ma and coworkers.^[23]

In order to effectively elaborate the ICT process, we developed a model as shown in Fig. 8. As far as the compound of p-PTPAPI was concerned, the linear connection would be benefit to the charge transfer between the strong D (TPA) and A (imidazole) units. In the meantime, another ICT process with the same connection also may be existed from phenanthrene to imidazole sectors. The good carries transfer and balance would be achieved based the compound of p-PTPAPI and the device will show good performance, which has been demonstrated. However, the strong the ICT will induce the red-shift emission, which will not be good for design materials with violet-blue emission.^[24] While the corresponding m-PTPAPI, the nonlinear connection between D and A units, the strong ICT will be effectively reduced, especially from phenanthrene to imidazole sectors. Therefore, the present emission will be shifted to violet. Meanwhile, the same constructing groups with p-PTPAPI, it can guarantee the good abilities of carries transfer and balance.

Conclusions

In conclusion, a couple of highly efficient deep-blue to violet-blue emitters, p-PATPA and m-PATPA, have been demonstrated by introducing D- π -A structure strategy to manage effectively their ICT processes. Their physical properties (PL, T_d , Φ , etc) were found to be good candidates for devices. Nondoped devices based on

them exhibit deep-blue light emissions with CIE coordinates of (0.15, 0.11) for p-PTPAPI and (0.16, 0.05) for m-PTPAPI at 100 cd/m², respectively. Interestingly, by introducing strong D and A in the compound of m-PTPAPI, we also achieved violet-blue emission by regulating the connecting mode to manage its ICT process. Its electroluminescence device shows good performance with EQE, CE, and PE of 2.39%, 0.78 cd/A, and 0.72 lm/W, respectively. Furthermore, at the high luminescence of 1000 cd/m², the EQE and CE of the m-PATPA device still remain high as 2.1% and 0.69 cd/A, indicative of a relatively low efficiency roll-off. Our results here successfully provide an efficient design strategy with strong D and A for violet-blue emitters.

Experimental section

General Procedures. ¹H NMR and ¹³C NMR spectra were determined in CDCl₃ with a Bruker DRX 400 MHz spectrometer. Chemical shifts (δ) were given relative to tetramethylsilane (TMS). The coupling constants (J) were reported in Hz. ESI-MS spectra were performed with a FINNIGAN Trace DSQ mass spectrometer at 70 eV. Elemental analyses were recorded with a Perkin-Elmer 2400 analyzer. Fluorescence emission spectra and decay curves of these samples were measured with a FLSP920 spectrophotometer. The film photoluminescence quantum yield was measured by the integrating sphere method. The absorption was recorded on a Hitachi U-3010 UV-vis spectrophotometer. The electrochemical properties of them were studied by cyclic voltammetry with a CHI600A analyzer. All starting materials were purchased from TCI and J&K Chemical companies. The reagents were obtained from sinopharm

chemical reagent Co. Ltd. and used without further purification. Experiment course was monitored by TLC. Column chromatography was carried out on silica gel (200-300 mesh).

Synthesis of 5-bromo-4'-(diphenylamino)-[1,1'-biphenyl]-3-carbaldehyde (2) (4-(diphenylamino)phenyl)boronic acid (1.445 g, 5.0 mmol), 3,5-dibromobenzaldehyde (2.641 g, 10 mmol) and Pd(PPh₃)₄ (50 mg, 0.10 mmol) were suspended in toluene (25 mL) and 10 mL 2M K₂CO₃. The reaction was stirred at 105 °C for 8 h and cooled to room temperature. The mixture solution was added 20 mL brine and then extracted with CH₂Cl₂ (40 mL), washed with water (2 x 20 mL), dried (MgSO₄) and evaporated to dryness. After drying under vacuum, then, it was purified by dichloromethane/petroleum ether (1:3) as an eluent to afford light yellow solid, Yield: 1.168 g, 54.6%. FTIR (KBr, cm⁻¹): 3095, 3068, 2942, 2918, 2894, 2866, 1698, 1499, 1506, 1409, 1392, 744; ¹H NMR(CDCl₃, 400 MHz, ppm) δ:10.02 (s, 1H), 7.97 (t, 3H, *J* = 14.8 Hz), 7.48 (d, 2H, *J*=8.66 Hz), 7.32 (t, 4H, *J*=7.42 Hz), 7.18 (d, 6H, *J*=8.67 Hz), 7.10 (t, 2H, *J*=7.42 Hz); EI-MS (m/z): 430.3 (M⁺+H), 428.1 (M⁺+H); Anal. Calcd for C₂₅H₁₈BrNO: C, 70.10; H, 4.24; N, 3.27; Found: C, 70.12; H, 4.18; N, 3.32.

Synthesis of 4'-(diphenylamino)-5-(phenanthren-9-yl)-[1,1'-biphenyl]-3-carbaldehyde (3) 5-bromo-4'-(diphenylamino)-[1,1'-biphenyl]-3-carbaldehyde (1.071 g, 2.5 mmol), phenanthren-9-ylboronic acid (0.666 g, 3 mmol) and Pd(PPh₃)₄ (25 mg, 0.05 mmol) were suspended in toluene (20 mL), 5 mL ethanol and 5 mL 2M K₂CO₃. The reaction was stirred at 105 °C for 12 h and cooled to room temperature. The mixture solution was added 10 mL brine and then extracted with CH₂Cl₂ (20 mL), washed with water

(2 x 10 mL), dried (MgSO₄) and evaporated to dryness. After drying under vacuum, then, it was purified by dichloromethane/ petroleum ether (1:1) as an eluent to afford light yellow solid, Yield: 1.084 g, 82.6%. FTIR (KBr, cm⁻¹): 3098, 3083, 3068, 2933, 2908, 2877, 2833, 1689, 1501, 1403, 1392, 1322, 732; ¹H NMR(CDCl₃, 400 MHz, ppm) δ:10.19 (s, 1H), 8.84 (d, 1H, *J*=7.99 Hz), 8.78 (d, 1H, *J*=8.17 Hz), 8.22 (s, 1H), 8.04 (d, 2H, *J*=15.25 Hz), 7.94 (d, 2H, *J*=8.29 Hz), 7.78 (s, 1H), 7.73 (t, 2H, *J*=8.30 Hz), 7.67 (t, 1H, *J*=7.32 Hz), 7.61 (t, 3H, *J*=8.43 Hz), 7.31 (t, 4H, *J*=7.92 Hz), 7.19 (t, 6H, *J*=7.42 Hz), 7.09 (t, 2H, *J*=7.71 Hz); EI-MS (m/z): 525.3 (M⁺); Anal. Calcd for C₃₉H₂₇N: C, 89.11; H, 5.18; N, 2.66; Found: C, 89.20; H, 5.19; N, 2.65.

Synthesis of 4'-(1-(4-bromophenyl)-1H-phenanthro[9,10-d]imidazol-2-yl)-N,N-diphenyl-[1,1'-biphenyl]-4-amine (5) A mixture of 4-bromoaniline (4.310 g, 25 mmol), phenanthrene-9,10-dione (1.041 g, 5 mmol), 4'-(diphenylamino)-[1,1'-biphenyl]-4-carbaldehyde (1.047 g, 4 mmol), ammonium acetate (1.694 g, 22 mmol), and acetic acid (40 mL) was heated for 12 h under argon at 125 °C. After cooled and filtered, the residue was purified by column chromatography with dichloromethane/ petroleum ether (1:1) to obtain a white powder. Yield, 1.426 g, 51.5%; FTIR (KBr, cm⁻¹): 3023, 3015, 2912, 2898, 1608, 1501, 1459, 1421, 1387, 733; ¹H NMR(CDCl₃, 400 MHz, ppm) δ:8.91 (d, 1H, *J*=8.06 Hz), 8.80 (d, 1H, *J*=8.23 Hz), 8.72 (d, 1H, *J*=8.75 Hz), 7.76 (d, 3H, *J*=7.89 Hz), 7.68 (t, 1H, *J*=7.53 Hz), 7.61 (d, 2H, *J*=7.59 Hz), 7.55 (d, 3H, *J*=8.16 Hz), 7.50 (d, 2H, *J*=8.25 Hz), 7.43 (d, 2H, *J*=7.84 Hz), 7.36-7.24 (m, 6H), 7.15 (d, 6H, *J*=7.43 Hz), 7.07 (t, 2H, *J*=7.02 Hz); EI-MS (m/z): 691.3, 693.2 (M⁺); Anal. Calcd for C₄₅H₃₀BrN: C, 78.03; H, 4.37; N, 6.07; Found: C, 78.11; H,

4.41; N, 6.09.

Synthesis of 3'-(phenanthren-9-yl)-N,N-diphenyl-5'-(1-phenyl-1H-phenanthro [9,10-d]imidazol-2-yl)-[1,1'-biphenyl]-4-amine (m-PTPAPI) A mixture of aniline (2.165 g, 12.5 mmol), phenanthrene-9,10-dione (0.521 g, 2.5 mmol), 4'-(diphenylamino)-5-(phenanthren-9-yl)-[1,1'-biphenyl]-3-carbaldehyde (1.051 g, 2 mmol), ammonium acetate (0.847 g, 11 mmol), and acetic acid (20 mL) was heated for 12 h under argon at 125 °C. After cooled and filtered, the residue was purified by column chromatography with dichloromethane/ petroleum ether (2:1) to obtain a white powder. Yield, 1.191 g, 75.5%; FTIR (KBr, cm^{-1}): 3043, 3032, 2893, 2881, 1601, 1531, 1488, 1392, 742; ^1H NMR (400MHz, CDCl_3): δ 8.91 (d, 1H, $J=7.91$ Hz), 8.87 (d, 2H, $J=7.92$ Hz), 8.74-8.70 (m, 2H), 7.99 (s, 1H), 7.88 (d, 1H, $J=7.90$ Hz), 7.80 (d, 1H, $J=8.79$ Hz), 7.77-7.61 (m, 12H), 7.54-7.50 (m, 3H), 7.43(d, 2H, $J=8.79$ Hz), 7.30-7.24 (m, 6H), 7.16-7.12 (m, 6H), 7.05 (t, 2H, $J=7.91$ Hz); ^{13}C NMR (100MHz, CDCl_3): δ 147.6, 141.2, 140.6, 138.1, 134.0, 131.5, 130.9, 130.6, 130.4, 130.1, 129.4, 129.3, 128.7, 127.9, 127.7, 126.8, 127.7, 126.5, 126.3, 124.5, 124.2, 123.7, 123.1, 122.9, 122.5, 120.9; EI-MS (m/z): 789.2 (M^+); Anal. Calcd for $\text{C}_{59}\text{H}_{39}\text{N}_3$: C, 89.70; H, 4.98; N, 5.32; Found: C, 89.74; H, 4.77; N, 5.49.

Synthesis of 4'-(1-(4-(phenanthren-9-yl)phenyl)-1H-phenanthro[9,10-d]imidazol-2-yl)-N,N-diphenyl-[1,1'-biphenyl]-4-amine (p-PTPAPI) phenanthren-9-ylboronic acid (0.555 g, 2.5 mmol), 4'-(1-(4-bromophenyl)-1H-phenanthro[9,10-d]imidazol-2-yl)-N,N-diphenyl-[1,1'-biphenyl]-4-amine (1.384 g, 2 mmol) and $\text{Pd}(\text{PPh}_3)_4$ (20 mg, 0.04 mmol) were suspended in toluene (20 mL), 4 mL ethanol and 8 mL 2M K_2CO_3 . The

reaction was stirred at 105 °C for 12 h and cooled to room temperature. The mixture solution was added 15 mL brine and then extracted with CH₂Cl₂ (30 mL), washed with water (2 x 15 mL), dried (MgSO₄) and evaporated to dryness. After drying under vacuum, then, it was purified by dichloromethane/ petroleum ether (3:1) as an eluent to afford white solid, Yield: 1.327 g, 82.4%. FTIR (KBr, cm⁻¹): 3053, 3041, 2956, 2911, 1597, 1499, 1422, 1392, 725; ¹H NMR (400MHz, CDCl₃): δ 8.98 (br, 1H), 8.83 (t, 2H, *J*=7.27 Hz), 8.76 (t, 2H, *J*=9.29 Hz), 8.80-7.95 (m, 2H), 7.88 (s, 1H), 7.82-7.56 (m, 15H), 7.52 (d, 2H, *J*=8.57 Hz), 7.48 (d, 1H, *J*=8.00Hz), 7.41 (d, 1H, *J*=6.86 Hz), 7.30-7.25 (m, 4H), 7.14 (d, 6H, *J*=6.29 Hz), 7.05 (t, 2H, *J*=6.86 Hz); ¹³C NMR (100MHz, CDCl₃): δ 147.8, 147.5, 123.0, 121.3, 130.6, 130.2, 129.4, 129.1, 128.8, 128.5, 128.1, 127.7, 127.2, 126.8, 126.5, 126.2, 124.6, 124.3, 123.6, 123.3, 122.7, 121.0; EI-MS (*m/z*): 789.1 (M⁺); Anal. Calcd for C₅₉H₃₉N₃: C, 89.70; H, 4.98; N, 5.32; Found: C, 89.48; H, 5.01; N, 5.51.

Computational Details The geometric and electronic structure of them were optimized by Density functional theory (DFT) level of theory with the three-parameter Becke-style hybrid functional (B3LYP). The HOMO and LUMO energy levels are predicated by 6-31G (d,p) basis set. All of calculations about the molecule have been performed on the huge computer origin 2000 server centre using the Gaussian 03 program package. The compositions of molecular orbits were analysed using the GaussView 3.0 program.

Devices fabrication Before fabrication of the OLED devices, both of PTPAPI are purified by sublimation. The ITO-coated glass substrate was first immersed

sequentially in ultrasonic baths of acetone, alcohol and deionized water for 10 min, respectively, and then dried in an oven. The resistance of a sheet ITO is 10-15 Ω/\square . The devices were fabricated in a multi-source organic molecule gas deposition system. Different organic materials were deposited on the ITO-coated glass substrate according to the designed structure. LiF buffer layer and Al were deposited as a co-cathode under a pressure of 5×10^{-4} Pa. Electroluminescent spectra and commission international De L' Eclairage(CIE) coordination of these devices were measured by a PR655 spectra scan spectrometer. The luminescent brightness (L)-current (I)-voltage (V) characteristics were recorded simultaneously with the measurement of the EL spectra by combining the spectrometer through a Keithly model 2400 programmable voltage-current source. The layer thicknesses of the deposited materials were monitored in situ using a model FTM-V oscillating quartz thickness monitor made in Shanghai, China. All the measurements were carried out at room temperature under ambient conditions.

Acknowledgements.

This work was financial supported from National Natural Science Foundation of China (21102156, 51273209), the External Cooperation Program of the Chinese Academy of Sciences (No. GJHZ1219), the Natural Science Foundation of Ningbo (201401A6105063), Ningbo International Cooperation Foundation (2013D10013), and the Open Research Fund of State Key Laboratory of Polymer Physics and Chemistry (Changchun Institute of Applied Chemistry, Chinese Academy of Sciences) and State Key Laboratory of Luminescence and Applications (Changchun Institute of

Optics, Fine Mechanics and Physics, Chinese Academy of Sciences)

References and notes

- [1] Zhu MR, Yang CL. Blue fluorescent emitters: design tactics and applications in organic light-emitting diodes. *Chem Soc Rev* 2013; 42: 4963-4976.
- [2] Wang J, Lou X, Liu YQ, Zhao GZ, Islam A, Wang SD, Ge ZY. Controllable molecular configuration for significant improvement of blue OLEDs based on novel twisted anthracene derivatives. *Dyes Pigm* 2015; 118: 137-144.
- [3] Ouyang XH, Li XL, Ai L, Mi DB, Ge ZY, Su SJ. Novel “hot exciton” blue fluorophores for high performance fluorescent/phosphorescent hybrid white organic light-emitting diodes with superhigh phosphorescent dopant concentration and improved efficiency roll-off. *ACS Appl. Mater. Interfaces* 2015, 7, 7869-7877.
- [4] Tong QX, Lai SL, Chan MY, Zhou YC, Kwong HL, Lee CS, et al. Highly efficient blue organic light-emitting device based on a nondoped electroluminescent material. *Chem. Mater.* 2008, **20**, 6310-6312.
- [5] Chou HH, Chen YH, Hsu HP, Chang WH, Cheng CH. Synthesis of diimidazolylstilbenes as n-type blue fluorophores: alternative dopant materials for highly efficient electroluminescent devices. *Adv Mater* 2012; 24: 5867-5871.
- [6] Lee S, Kim S-O, Shin H, Yun H-J, Yang K, Kwon S-K, et al. Deep-blue phosphorescence from perfluoro carbonyl-substituted iridium complexes. *J Am Soc Chem* 2013; 135: 14321-14328.

- [7] Ye J, Chen Z, Fung, M-K, Zheng C, Ou X, Zhang X, et al. Carbazole/sulfone hybrid D- π -A structured bipolar fluorophores for high-efficiency blue violet electroluminescence. *Chem Mater* 2013; 25: 2630-2637.
- [8] Yu DH, Zhao FC, Zhang Z, Han CM, Xu H, Li J, et al. Insulated donor- π -acceptor systems based on fluorene-phosphine oxide hybrids for non-doped deep-blue electroluminescent devices. *Chem Commun* 2012; 48: 6157-6159.
- [9] Fisher AL, Linton KE, Kamtekar, KT, Pearson C, Bryce MR, Petty MC. Efficient deep-blue electroluminescence from an ambipolar fluorescent emitter in a single-active-layer device. *Chem Mater* 2011; 23: 1640-1642.
- [10] Ouyang XH, Li XL, Bai YQ, Mi DB, Ge ZY, Su SJ. Highly-efficient hybrid white organic light-emitting diodes based on a high radiative exciton ration deep-blue emitter with improved concentration of phosphorescent dopant. *RSC Adv* 2015; 5: 32298-32306.
- [11] Wu CH, Chien CH, Hsu FM, Shih PI, Shu CF. Efficient non-doped blue-light-emitting diodes incorporating an anthracene derivative end-capped with fluorene groups. *J Mater Chem* 2009; 19: 1464-1470.
- [12] Hosokawa C, Higashi H, Nakamura H., Kusumoto T. Highly efficient blue electroluminescence from a distyrylarylene emitting layer with a new dopant. *Appl Phys Lett* 1995; 67: 3853-3855.
- [13] Lo MY, Zhen C, Lauters M, Jabbour GE, Sellinger A. Organic-inorganic hybrids based on pyrene functionalized octavinylsilsesquioxane cores for application in OLEDs. *J Am Chem Soc* 2007; 129: 5808;

- [14] Ren XF, Li J, Holmes RJ, Djurovich PI, Forrest SR, Thompson ME. Ultrahigh energy gap hosts in deep blue organic electrophosphorescent devices. *Chem Mater* 2004; 16: 4743-4747.
- [15] Wang Z, Lu P, Chen S, Gao Z, Shen F, Zhang W, et al. Phenanthro[9,10-d]imidazole as a new building block for blue light emitting materials. *J Mater Chem* 2011; 21: 5451-5456.
- [16] Kowalski K, Long NJ, Kuimova MK, Kornyshev AA, Taylor AG, White AJP. Synthesis and characterisation of substituted diphenylamines-charge-transfer, donor-acceptor systems localised at water-oil interfaces. *New J Chem* 2009; 33: 598-606.
- [17] Tang S, Li WJ, Shen FZ, Liu DD, Yang B, Ma YG. Highly efficient deep-blue electroluminescence based on the triphenylamine-cored and peripheral blue emitters with segregative HOMO-LUMO characteristics. *J Mater Chem* 2012; 22: 4401-4408.
- [18] Zhang XY, Lin J, Ouyang XH, Liu Y, Liu XY, Ge ZY. Novel host materials based on phenanthroimidazole derivatives for highly efficient green phosphorescent OLEDs. *J Photochem Photobiol A* 2013; 268: 34-43.
- [19] Zhang XY, Xu Z, Ge ZY, Ouyang XH, Ji W. Tunable molecular configuration for significant enhancement of two-photon absorption based on novel octupolar benzoimidazole derivatives. *J Photochem Photobiol A* 2014; 290: 22-30.
- [20] Grabowski ZR, Rotkiewicz K, Rettig, W. Structural changes accompanying intramolecular electron transfer: Focus on twisted intramolecular charge-transfer states and structures. *Chem Rev* 2003; 103: 3899-4031.

- [21] Ouyang XH, Zhang XY, Ge ZY. Enhanced efficiency in nondoped, blue organic light-emitting diodes utilizing simultaneously local excitation and two charge-transfer exciton from benzimidazole-based donor-acceptor molecules. *Dyes Pigm* 2014; 103: 39-49.
- [22] Chiang CJ, Kimyonok A, Etherington MK, Griffiths GC, Jankus V, Turksroy F, et al. Ultrahigh efficiency fluorescent single and bi-layer organic light emitting diodes: the key role of triplet fusion. *Adv Funct Mater* 2013; 23:739-746.
- [23] Li WJ, Liu DD, Shen FZ, Ma DG, Wang ZM, Feng T, et al. A twisting donor-acceptor molecule with an intercrossed excited state for highly efficient, deep-blue electroluminescence. *Adv Funct Mater* 2012; 22: 2797.
- [24] Tao YT, Wang Q, Yang CL, Zhong C, Zhang K, Qin JG, et al. Tuning the optoelectronic properties of carbazole/oxadiazole hybrids through linkage modes: hosts for highly efficient green electrophosphorescence. *Adv Funct Mater* 2010; 20: 304-311.

Table Captions

Table 1. Physical data of p-PTPAPI and m-PTPAPI.

Table 2. Electroluminescent characteristics of the devices with the structure of ITO/HATCN (5 nm)/NPB (x nm)/TCTA (5 nm)/emitters (y nm)/TPBi (z nm)/LiF (1 nm)/Al (90 nm).

Table 1

Compounds	T_d (°C)	Abs (nm)	PL (nm)	Φ (%)	HOMO(eV) (electro/calculated)	LUMO(eV) (electro/calculated)	energy gap(eV) (electro/calculated)
p- PTPAPI	478	305,370	446	50.3	-5.3/-4.88	-2.57/-2.42	2.73/2.46
m- PTPAPI	475	310	410	36.9	-5.3/-4.97	-2.4/-2.11	2.9/2.86

Table 2

emitter	thickness x,y,z, (nm)	CIE (x,y)	L_{max} cd/m ²	η_c cd/A	η_p lm/W	η_e (%)	Devices @100 cd m ⁻²			Devices @1000 cd m ⁻²		
							η_c (cd/A)	η_p (lm/W)	η_e (%)	η_c (cd/A)	η_p (lm/W)	η_e (%)
p-PTPAPI	30, 30, 40	(0.16, 0.15)	11936	3.14	2.29	3.12	3.07	2.14	3.06	3.12	2.13	2.99
	60, 20, 50	(0.16, 0.15)	9076	2.87	1.49	2.89	2.66	1.40	2.65	2.87	1.19	2.62
	40, 20, 40	(0.15, 0.15)	10574	3.73	3.47	3.71	3.46	2.59	3.45	3.25	1.80	3.23
m-PTPAPI	30, 30, 40	(0.16, 0.05)	2425	0.65	0.34	1.99	0.61	0.30	1.93	0.64	0.24	1.68
	60, 20, 50	(0.16, 0.05)	2471	0.64	0.24	1.96	0.59	0.24	1.91	0.64	0.20	1.72
	40, 20, 40	(0.15, 0.05)	3126	0.78	0.72	2.39	0.78	0.51	2.37	0.69	0.28	2.10

Figure Captions

Fig. 1. TGA curves of p- PTPAPI and m- PTPAPI

Fig. 2. Cyclic voltammograms curves of p- PTPAPI and m- PTPAPI.

Fig. 3. Normalized UV absorption and photoluminescent spectra of p- PTPAPI and m- PTPAPI in film

Fig. 4. Fluorescence spectra of TPABBI and TPABBI in various polarity solvents; and solvent polarity (*f*) dependence of the fluorescence maxima of p- PTPAPI (insert Fig. a) and m-PTPAPI (insert Fig. b)

Fig. 5. Spatial distributions of HOMO and LUMO of p-PTPAPI and m- PTPAPI

Fig. 6. The electroluminescent (EL) spectra of p-PTPAPI (a) and m-PTPAPI (b) with different current densities

Fig. 7. The EL performance of p-PTPAPI and m-PTPAPI, (a) current density-voltage-luminance (J–V–L); (b) brightness-luminescent efficiencies curves; (c) brightness-power efficiencies curves; (d) brightness-external quantum efficiencies curves.

Fig. 8. The diagram of ICT process in the molecules of p-PTPAPI and m-PTPAPI

Scheme Captions

Scheme 1. The synthetic routes of p-PTPAPI and m- PTPAPI

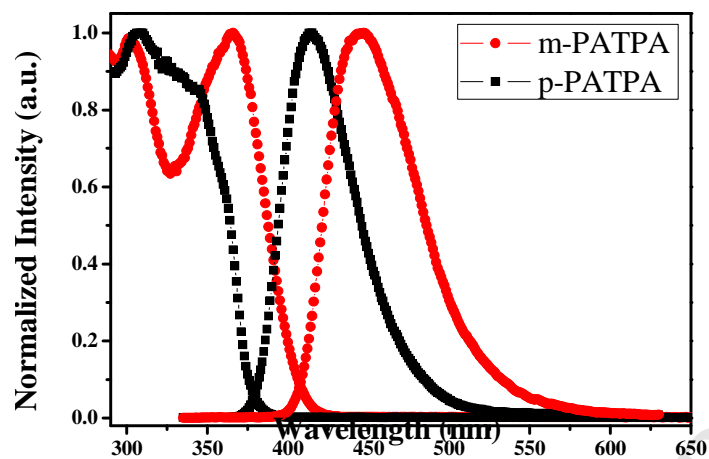


Fig. 1

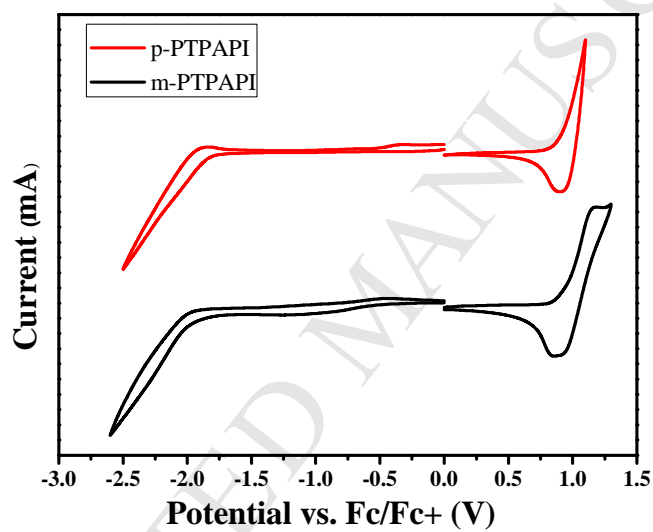


Fig. 2

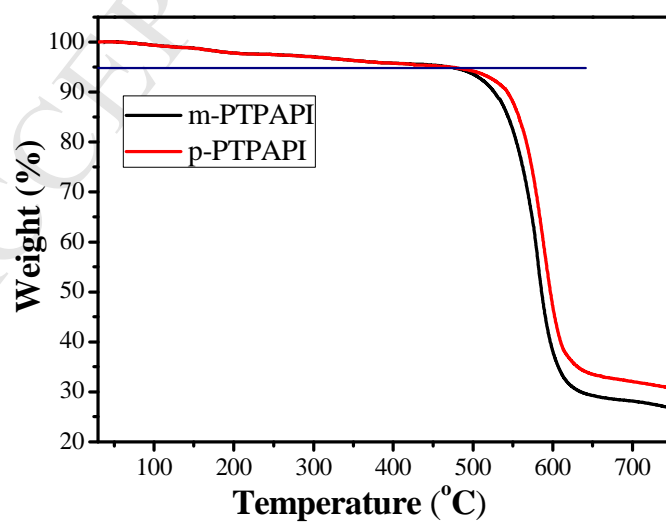


Fig. 3

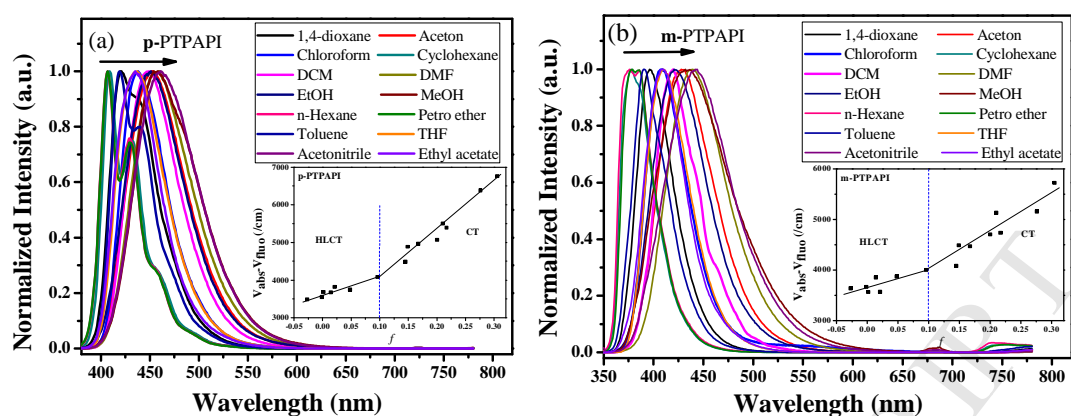


Fig. 4

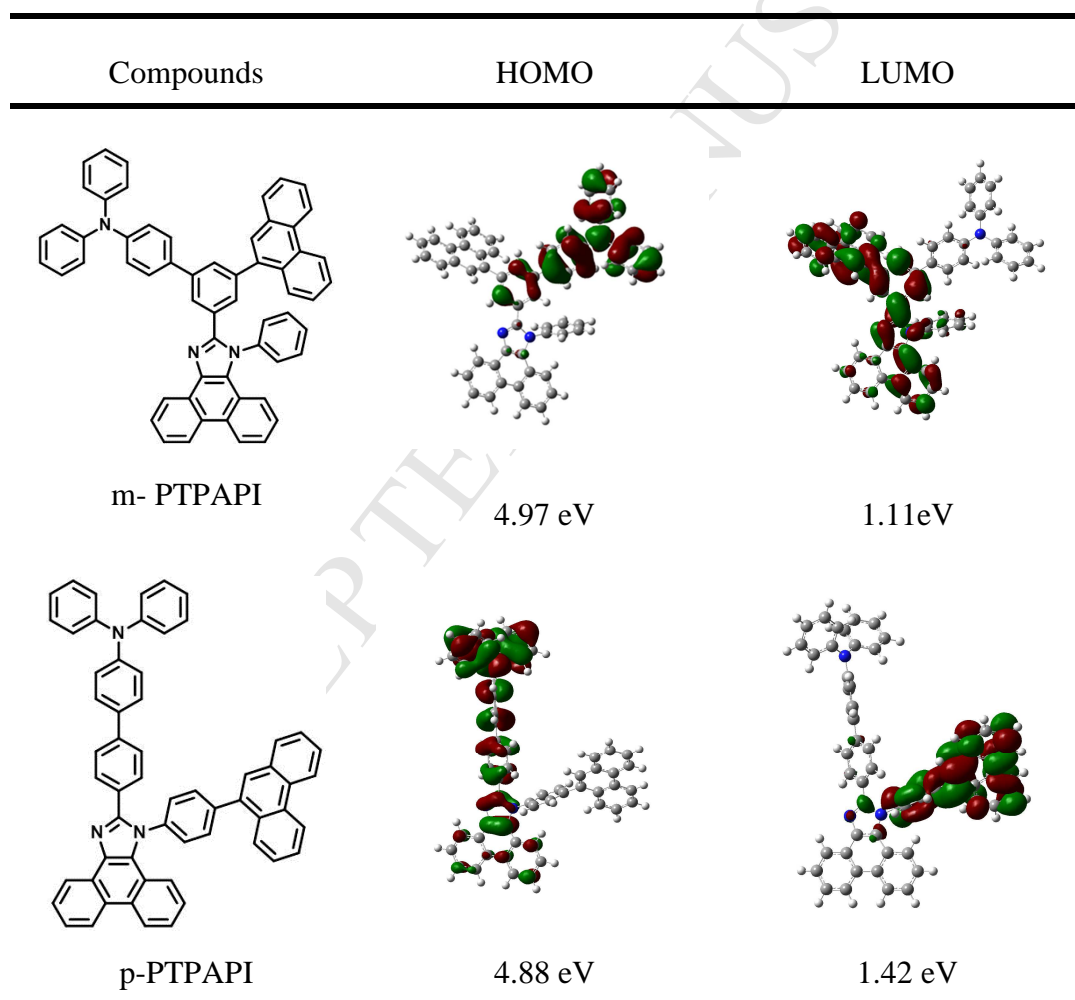


Fig. 5

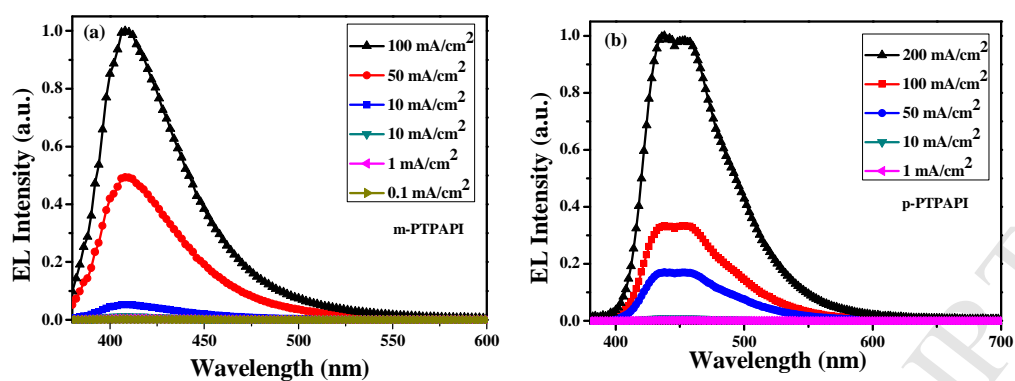


Fig. 6

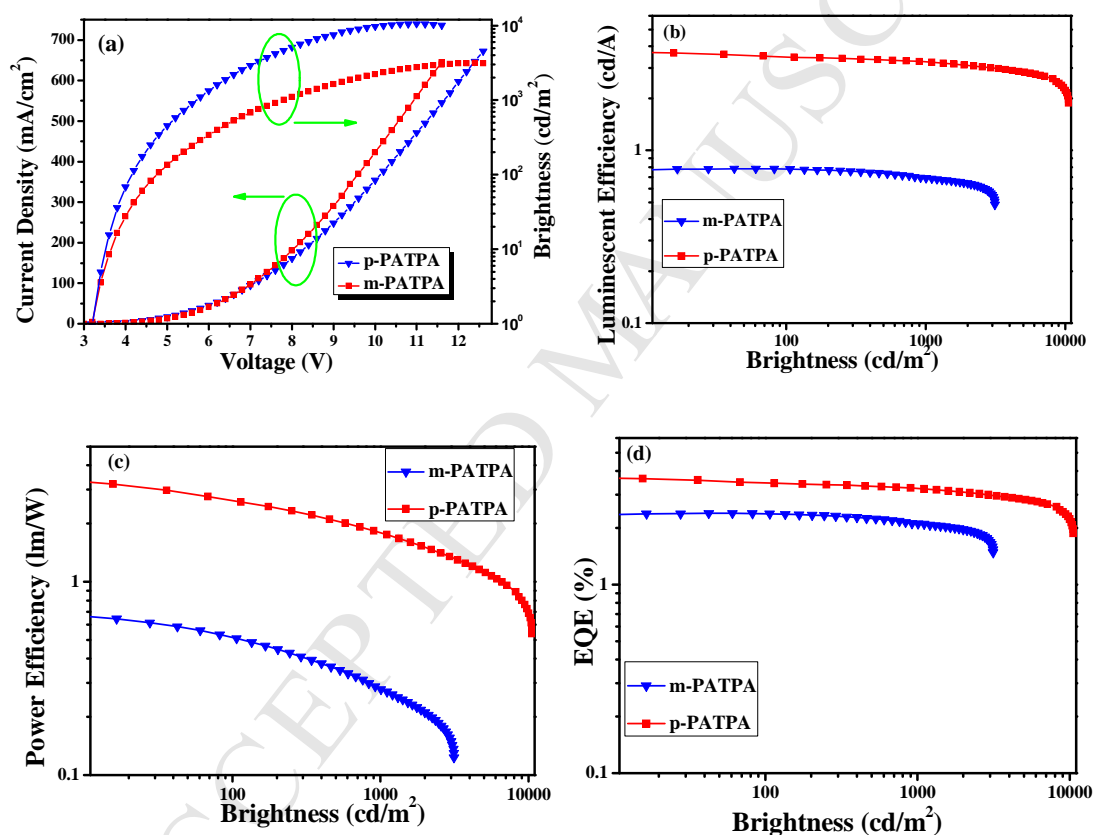


Fig. 7

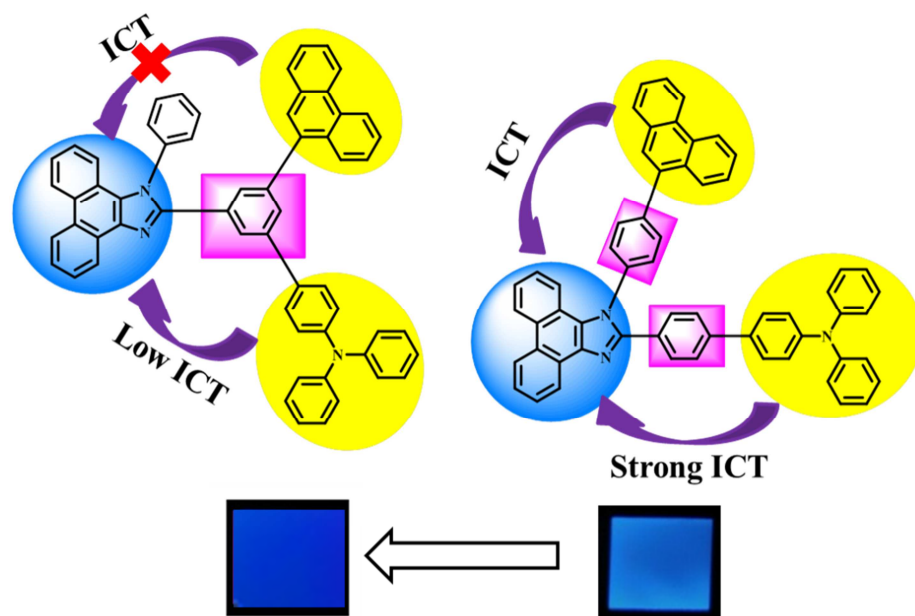
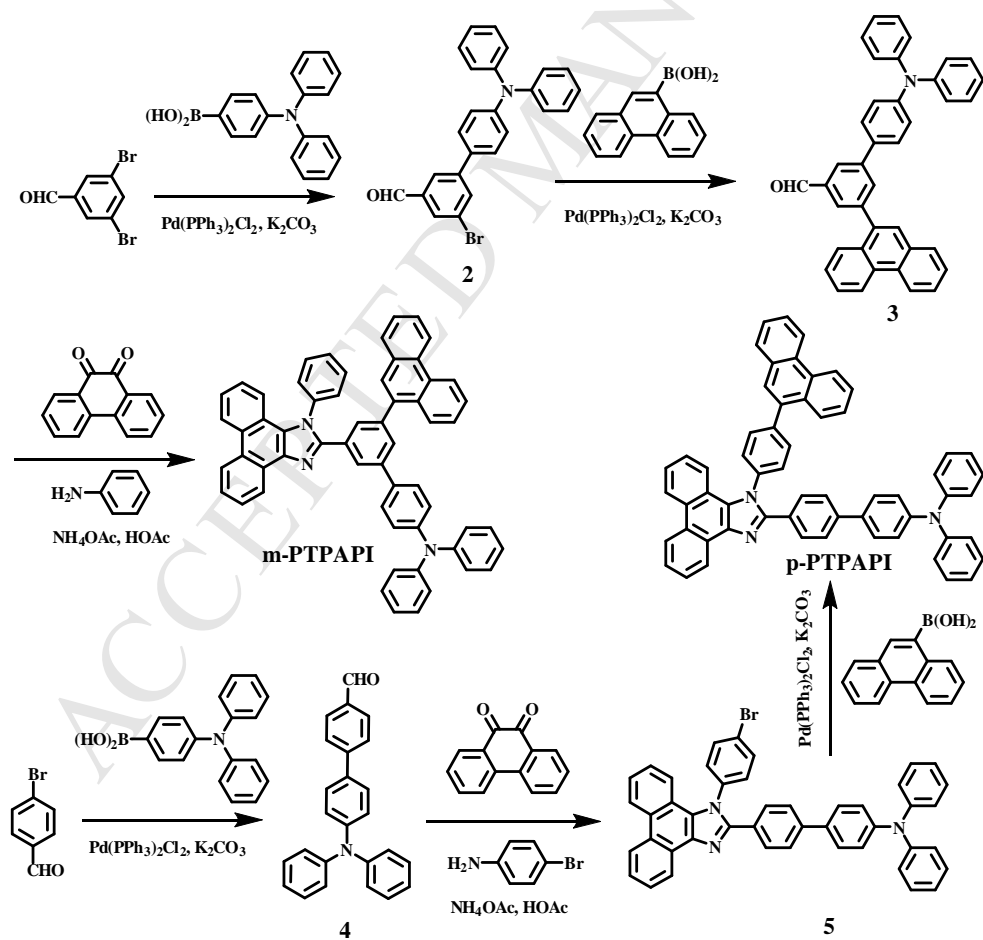


Fig. 8



Scheme 1

Research highlights

► Novel phenanthrene isomers were synthesized and characterized. ► Management of their intramolecular charge transfer (ICT) processes for violet-blue emitters ► The results were found to be good candidates as emitters for organic light emitting diodes (OLEDs) ► The devices exhibit violet-blue light emissions with CIE coordinates of (0.16, 0.05) for m-PATPA at 100 cd/m², respectively. ► The results provide an efficient design strategy with strong donor (D) and acceptor (A) for violet-blue emitters.